https://doi.org/10.48048/tis.2024.6162

A Numerical Investigation of Hydro-Magnetic Mixed Convection Flow of Viscous Dissipative Fluid in a Channel Filled with Porous Material

Samaila Kenga-kwai Ahmad[1], Yakubu Bello[2,*] and Muhammed Murtala Hamza[1]

[1]Department of Mathematics, Faculty of Physical and Computing Science, Usmanu Danfodiyo University, Sokoto State 2346, Nigeria
[2]Department of Mathematics, Faculty of Science, Air Force Institute of Technology, Kaduna State 2104, Nigeria

([*]Corresponding author's e-mail: yakubabello1988@gmail.com)

Received: 30 September 2022, Revised: 27 October 2022, Accepted: 3 November 2022, Published: 5 October 2023

Abstract

The purpose of this paper is to inspect the unsteady MHD mixed convective Couette flow of viscous dissipative fluid in a vertical channel filled with porous material. The steady state analytical solutions of temperature, velocity, frictional force and heat transfer rate are obtained using the Homotopy perturbation method (HPM). The implicit finite difference technique is used to solve the transient leading equations numerically. Plots and tables with the dynamic flow parameters and dimensionless variables are displayed. During this computation, it was found that raising the Darcy parameter (*Da*) and the mixed convection (*Gre*) parameters both push the fluid flow upwards, but increasing the magnetic field's values had the opposite effect (*M*).

Keywords: Mixed convection, Couette flow, Viscous dissipation, MHD, Porous material, Homotopy perturbation method

Introduction

Mixed convection refers to a variety of circumstances when similar orders of magnitude coexist between forced and free convection. We can list isotherm jets, sluggish flows in pipes (like in water radiators) or along walls, and atmospheric flows and currents as instances of this diversity (more broadly, numerous highly isothermal flows). For many years, mixed convection in micro-channels has been used to treat heat transport (Avci and Aydin [1]; Avramenko [2]). As a result, Jha *et al.* [3] conducted a theoretical analysis on the fully developed hydro-magnetic fluid in a vertical micro-channel that generates and absorbs heat and is affected by hall and ion-slip phenomena. When heat generation and absorption is present, increasing ion-slip and hall current parameters can increase primary velocity and thermal gradient, but their effect on velocity is opposite in the secondary direction. In a cylinder speed cavity that was differentially heated, Khanafer *et al.* [4] conducted mixed convection heat transfer. They discovered that at high values of the cylinder's rotational speed, the Reynolds number (Re) and the Richardson number (Ri), the average Nusselt number improved. Additionally, this model demonstrated that the heat transfer rate was similar to the cylinder speed values for high Richardson numbers. In their analysis of mixed convection flow of a viscous dissipating fluid through a channel moving in the opposite direction, Gupta *et al.* [5] discovered that the velocity of a fluid increases due to increases in Grashof number, suction parameter, and permeability parameter, whereas the thermal gradient decreases with increases in suction parameter or Prandtl number, while it rises due to increases in the magnetic parameter and dissipating parameter. An experimental investigation into the thermal conductivity of a nanofluid made of MWCNT-CuO/water was given by Masoud *et al.* [6]. Xu and Sun [7] put 4th a theoretical investigation of a hybrid nanofluid in a vertical microchannel with mixed convection. They claimed that the dynamic and thermal behaviors were significantly influenced by the nanoparticle volumetric fractions. They also showed that the volume proportions of nanoparticles and Ri would boost the average heat transfer rate. The mixed convection of nano-fluids in circular micro-channels was studied by Manay and Mandev [8]. They discovered that increasing the volume percentage of silicon dioxide nanoparticles in suspension increased the rate of heat transfer. As a result, it would get smaller independent of the Reynolds number.

The study of viscous dissipation in both free and mixed convections has sparked various fascinating research efforts due to its potential applications in lubricating industries, nuclear reactor cooling, electric appliance cooling, and so on. Viscous dissipation is a critical feature that occurs when fluid particles contact

and generate internal mechanical energy. This type of energy dissipation has a substantial action on the hydrodynamic and thermodynamic behavior of fluids. Viscous dissipation is unavoidable in the lubrication industry, and Gebhart [9] was the first to analyze the influence of viscous dissipation on natural convection. He discovered that in a steady natural convection, viscous dissipation cannot be ignored in a fluid with a high Prandtl number or a fluid with strong gravitational forces. Since then, many researchers have studied heat transmission through mixed convection and viscous dissipation on heat generating and absorbing fluids in a variety of geometries. Ajibade and Umar [10] presented an analytical investigation on the influence of heat generating/absorbing fluid, viscous dissipation and suction/injection on a steady hydro-magnetic free convection couette flow in this regard. Ajibade and Umar [11] followed up on their previous work by discussing the consequences of viscous dissipation and suction/injection on a steady MHD mixed convection fully developed laminar flow of heat generating/absorbing fluid through vertical parallel porous plates channel using the homotopy perturbation method. Convection heat transfer flow between vertical parallel plates with time-periodic boundary layer and the impact of viscous dissipation was investigated by Jha and Ajibade [12]. They demonstrated that when the fluid's Prandtl number is low, dissipation heating in the channel raises the fluid temperature above the plate temperature. Jha and Ajibade [13] carefully examined free convective unsteady the couette flow of heat source/sink. Their findings demonstrate that when heat absorption increases, heat transfer rates on moving plates increase while those on stationary plates drop. Ajibade and Thomas [14] investigated the entropy generation and irreversibility analysis resulting from steady mixed convection flow in a vertical porous channel. They discovered that as mixed convection increases, the velocity profile also rises, although temperature shows the opposite trend. Mohamed [15] investigated the mixed convection flow of a micro-polar fluid from an unsteady stretched surface under viscous dissipation effect. He came to the conclusion that as the Eckert number rises, the velocity and temperature profiles do as well. Mohamed [16] also investigated viscous dissipation and varying viscosity over a vertical stretched surface with mixed convection heat transfer. He demonstrated that the mixed convection parameter has a more noticeable impact on the fluid acceleration and thermal distribution in the steady flow than it does in the unsteady flow. He also found that when the mixed convection parameter's strength grows, so do the flow and temperature fields. Dulal and Hiranmony [17] investigated the impact of temperature-dependent viscosity and variable thermal conductivity on non-Darcy mixed convective species diffusion in magneto-hydrodynamics (MHD) over a stretching sheet. Because the mixed convection rises, the layer thickness at the thermal boundary falls, they came to the conclusion that the fluid velocity goes up*ward* as the mixed convective parameter increases while the temperature profile drops.

The use of porous media in micro-channels and heat exchangers is a technique that is becoming more and more intriguing for enhancing convection heat transfer characteristics. A porous medium, according to Mahmoodi *et al.* [18], is a solid matrix with void spaces called pores that are linked by a system of channels through which fluid can flow. Numerous applications such as the storage of radioactive nuclear waste, geothermal extraction, transpiration cooling, filtration, crude oil extraction, heating and cooling in buildings, and many others, involve the flow of fluid and the transmission of heat within channels saturated with porous medium. Using Hamming's predictor-corrector approach, Joshi and Gebhart [19] offered a technical remark on the mixed-convection mechanism through a heat flux surface with a porous material. In order to get numerical results with free-stream velocity and modest amplitude fluctuations in the wall temperature embedded in a porous material, Chamkha [20] used the Kellerbox technique. Chamkha *et al.* [21] analyzed the action of a transverse magnetic field on mixed-convection events over a semi-infinite permeable vertical plate in a porous medium with uniform heat flux. The MHD convection flow of Casson fluid in micro-channels including porous material was discussed by Gireesha and Sindhu [22]. When Noor *et al.* [23] used network simulation method solutions to analyze time-dependent hydro-magnetic radiative fluid flow over an inclined porous plate with heat and mass permeability, they found that the fluid momentum tended to rise or fall gradually towards the plate and then diminish or grow slowly away from the plate. The temperature of the fluid has been reported to exhibit the same tendency.

The goal of this research is to analyze unsteady hydro-magnetic mixed convective flow of viscous dissipative fluid in a channel embedded with porous medium. The leading equations of the current flow problem are nonlinear and coupled, so that deriving closed-form solutions is an arduous assignment. Therefore, these issues are solvable by numerical techniques or some approximate solution procedures. The perturbation method is one of the most efficient procedures. However, the perturbation method’s solutions are limited to modest perturbation parameters. To circumvent this limitation, another method known as the Homotopy perturbation technique was developed. He [24] used the method to solve linear, nonlinear, and coupled equations in partial or ordinary form. He [25] examined a coupling method for non-linear problems using homotopy technique and a perturbation technique. Later, He [26] presented a new nonlinear analytical

scheme using the Homotopy perturbation method. Zigta [27] reported an important results which show that an increment in the radiation absorption parameter and permeability of porous medium results in an increment of the temperature profile. Moreover, an increment in the Prandtl number, Eckert number and dynamic viscosity results in a decrement of the temperature profile. An increment in suction velocity results in a decrement of the velocity profile. An increment in the Schmidt number, chemical reaction parameter and kinematic viscosity results in a decrement of the concentration profile, in his paper tittled mixed convection on MHD flow with thermal radiation, chemical reaction and viscous dissipation embedded in a porous medium. Recent works have been compared with the present work; an excellent agreement is found when magnetic field is set to be 0 and Darcy parameter is set to be 1,000, the work of Ajibade and Umar [10] is recovered. In addition, results derived from this study can be very helpful to designers in improving the behavior of mechanical systems when viscous dissipation is involved and heat transfer in channels as it is in combustion in auto piston

Materials and methods

Consider the case when a vertical pair of parallel plates are experiencing a time-dependent fully developed flow of a chemically reactive fluid with one plate moving and the other fixed (see **Figure 1**). While the plate at y' = 0 is heated, the plate at y' = h is maintained at room temperature.

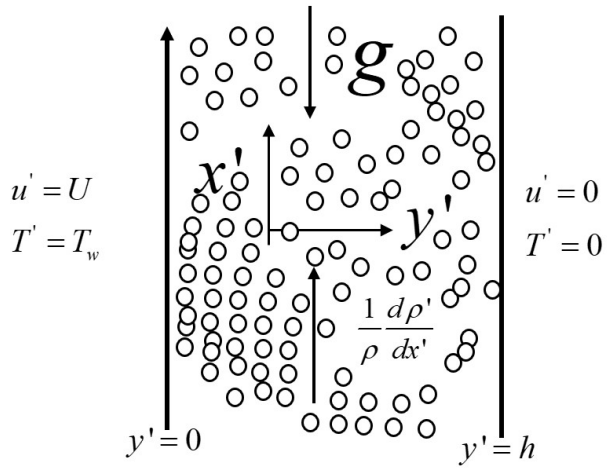

Figure 1 Schematic diagram.

In the presence of viscous dissipation, the fluid flow is subjected to free and forced convection; additionally, the flow is considered to be in a direction of x' and y' normal to the plates. Internal energy is produced as a result of fluid particle contact, and the thermos-physical properties are supposed to be constants in the linear momentum equation, as approximated by the Boussinesq approximation. The physical equations that describe the scenario are considered to be as follows:

$$\frac{\partial u'}{\partial t'} = \nu \frac{\partial^2 u'}{\partial y'^2} + g\beta\left(T' - T_0\right) - \frac{\nu\beta^2 u'}{\rho} - \frac{\nu u'}{\kappa} - \frac{1}{\rho}\frac{\partial p'}{\partial x'} \tag{1}$$

$$\frac{\partial T'}{\partial t'} = \frac{\kappa}{\rho c_p}\frac{\partial^2 T'}{\partial y'^2} - \frac{Q_0}{\rho c_p}\left(T' - T_2\right) + \frac{\nu}{c_p}\left(\frac{\partial u'}{\partial y'}\right)^2 \tag{2}$$

where y' and x' are the dimensional distances along and perpendicular to the plate. u' and T' are the dimensional velocity, and temperature. Q_0, ν, k, ρ, c_p, β, and g are the dimensional heat source/sink coefficient, kinetic viscosity, thermal conductivity, density, specific heat at constant pressure, thermal expansion coefficient, and acceleration due to gravity of the fluid, respectively. The 1st and 2nd terms at the right hand side of Eq. (1) are the viscosity, thermal buoyancy, magnetic field, porous medium and pressure effect of the fluid. Also, the 1st and 2nd terms at the left hand side of Eq. (2) are thermal conductivity, heat source/sink, and viscous dissipation effect of the fluid, while at the left hand side in Eq. (1) is the unsteady

velocity and unsteady temperature in Eq. (2). We assume that the appropriate boundary conditions of the model are:

$$\begin{aligned} &u' = U, \quad T' = T_w, y' = 0 \\ &u' = 0, \quad T' = T_0, \quad y' = h \end{aligned} \tag{3}$$

where U, T_w and T_0 are the velocity of the moving plate, temperature of the heated and cold plate respectively. The following are the dimensionless quantities used:

$$u = \frac{u^*}{U}, \quad y = \frac{y'}{h}, \quad T = \frac{T' - T_0}{T_w - T_0}, \qquad x = \frac{x'v}{Uh^2}, \qquad P = \frac{P'}{\rho U^2}$$

$$M = \frac{\nu \beta_0{}^2 h^2}{\nu}, \qquad Da = \frac{\kappa}{h^2} \tag{4}$$

where Gr is the thermal Grashof number, Re is the Reynold number, Pr is the Prandtl number, Ec is Eckert number, S is heat source/sink parameter, $Gr = Gre$ is mixed convection parameter, and $\mathrm{EcPr} = \mathrm{Br}$ Brinkman number.

$$Gr = \frac{g\beta(T_w - T_0)h^3}{\nu^2}, \qquad \mathrm{Re} = \frac{Uh}{\nu}, \qquad \mathrm{Pr} = \frac{\nu}{\alpha}, S = \frac{Q_0 h^2}{k}, Ec = \frac{U^2}{c_p(T_w - T_0)}, Gre = \frac{Gr}{\mathrm{Re}}, Ec\,\mathrm{Pr} = Br$$

Using the dimensional quantities above, the basic field Eqs. (1) and (2) can be written in dimensionless form as:

$$\frac{\partial u}{\partial t} = \frac{\partial^2 u}{\partial y^2} + GreT - \left(M + \frac{1}{Da}\right)u - \frac{\partial p}{\partial x} \tag{5}$$

$$\mathrm{Pr}\frac{\partial T}{\partial t} = \frac{\partial^2 T}{\partial y^2} + Br\left(\frac{\partial u}{\partial y}\right)^2 - ST \tag{6}$$

and the boundary conditions are:

$$\left.\begin{aligned} &u = 1, \quad T = 1, \quad y = 0 \\ &u = 0, \quad T = 0, \quad y = 1 \end{aligned}\right\} \tag{7}$$

By equating $\frac{\partial u}{\partial t} = 0$ and $\mathrm{Pr}\frac{\partial T}{\partial t} = 0$, we have:

$$\frac{d^2 u}{dy^2} + GreT - \left(M + \frac{1}{Da}\right)u - \frac{dp}{dx} = 0 \tag{8}$$

$$\frac{d^2 T}{dy^2} + Br\left(\frac{du}{dy}\right)^2 - ST = 0 \tag{9}$$

Steady state solution

To solve our problem, HPM has been used. Convex homotopy of the momentum and energy equations has been constructed. Therefore, the momentum Eq. (8) is transformed as:

$$H(u,p) = (1-p)\left[\frac{d^2 u}{dy^2} - \frac{d^2 v_0}{dy^2}\right] + p\left[\frac{d^2 u}{dy^2} + GreT - \left(M + \frac{1}{D}\right)u - \frac{dp}{dx}\right] = 0 \tag{10}$$

Since the 0th order is linear and is solvable without any recourse to initial approximation, therefore, Eq. (7) can be expressed as:

$$\frac{d^2u}{dy^2} = p\left[\frac{dp}{dx} + \left(M + \frac{1}{D}\right)u - GreT\right] \tag{11}$$

Setting u and T as infinite series such that:

$$\begin{aligned} u &= u_0 + pu_1 + P^2u_2 + \cdots \\ T &= T_0 + pT_1 + P^2T_2 + \cdots \end{aligned} \tag{12}$$

Substituting Eq. (13) into Eq. (12), we have:

$$\begin{aligned} &\frac{d^2u_0}{dy^2} + p\frac{d^2u_1}{dy^2} + P^2\frac{d^2u_2}{dy^2} + \cdots \qquad = p\frac{dP}{dx} + p\left(M + \frac{1}{Da}\right)u_0 + p^2\left(M + \frac{1}{Da}\right)u_1 + \cdots \\ &-pGreT_0 - p^2GreT_1 - \cdots \end{aligned} \tag{13}$$

Comparing the coefficients of $p^0, p^1, p^2, \cdots,$ the equation is split as:

$$p^0 : \frac{d^2u_0}{dy^2} = 0 \tag{14}$$

$$p^1 : \frac{d^2u_1}{dy^2} = \frac{dP}{dx} + \left(M + \frac{1}{Da}\right)u_0 - GreT_0 \tag{15}$$

$$p^2 : \frac{d^2u_1}{dy^2} = \left(M + \frac{1}{Da}\right)u_1 - GreT_1 \tag{16}$$

Similarly, Eq. (8) is transformed as:

$$\frac{d^2T}{dy^2} = p\left[ST - Br\left(\frac{du}{dy}\right)^2\right] \tag{17}$$

Substituting Eq. (13) into Eq. (18), we have:

$$\begin{aligned} &\frac{d^2T_0}{dy^2} + p\frac{d^2T_1}{dy^2} + P^2\frac{d^2T_2}{dy^2} + \cdots \qquad = pST_0 + p^2ST_1 + p^3ST_2 + \cdots \\ &-pBr\left(\frac{du_0}{dy}\right)^2 - 2p^2Br\frac{du_0}{dy}\frac{du_1}{dy} + \cdots \end{aligned} \tag{18}$$

Comparing the coefficients of $p^0, p^1, p^2, \cdots,$ the equation is split as:

$$p^0 : \frac{d^2T_0}{dy^2} = 0 \tag{19}$$

$$p^1 : \frac{d^2T_1}{dy^2} = ST_0 - Br\left(\frac{du_0}{dy}\right)^2 \tag{20}$$

$$p^2 : \frac{d^2T_2}{dy^2} = ST_1 - 2Br\frac{du_0}{dy}\frac{du_1}{dy} \tag{21}$$

And transformed boundary conditions for momentum and energy equations are:

$$\begin{aligned} &\mathrm{u}_0(0)=1, && \mathrm{u}_1(0)=0, && \mathrm{u}_2(0)=0 \\ &\mathrm{u}_0(1)=0, && \mathrm{u}_1(1)=0, && \mathrm{u}_2(1)=0 \end{aligned} \tag{22}$$

$$\begin{aligned} &T_0(0)=1, && T_1(0)=0, && T_2(0)=0 \\ &T_0(1)=0, && T_1(1)=0, && T_2(1)=0 \end{aligned} \tag{23}$$

Solving for Eqs. (15) and (20) we have:

$$\mathrm{u}_0 = \mathrm{A}_1 y + A_2 \tag{24}$$

$$T_0 = \mathrm{B}_1 y + B_2 \tag{25}$$

Applying the boundary conditions for $\mathrm{u}_0(0)=1$, $\mathrm{u}_0(1)=0$ and $T_0(0)=1$, $T_0(1)=0$, respectively we have:

$$\mathrm{u}_0 = 1 - y \tag{26}$$

$$T_0 = 1 - y \tag{27}$$

From 1st order, we solve the Eqs. (16) and (21) to have:

$$u_1 = \frac{y^2}{2}\frac{dp}{dx} - Gre\left(\frac{y^2}{2}-\frac{y^3}{6}\right) + \left(M+\frac{1}{Da}\right)\left(\frac{y^2}{2}-\frac{y^3}{6}\right) + A_3 y + A_4 \tag{28}$$

$$T_1 = S\left(\frac{y^2}{2}-\frac{y^3}{6}\right) - Br\frac{y^2}{2} + B_3 y + B_4 \tag{29}$$

Applying boundary conditions $\mathrm{u}_1(0)=0$, $\mathrm{u}_1(1)=0$ and $T_1(0)=0$, $T_1(1)=0$

$$A_3 = \frac{Gre}{3} - \frac{1}{3}\left(M+\frac{1}{Da}\right) - \frac{1}{2}\frac{dp}{dx}, \quad A_4 = 0, \quad B_3 = \frac{Br}{2} - \frac{S}{3}, \quad B_4 = 0$$

$$u_1 = \frac{y^2}{2}\frac{dp}{dx} - Gre\left(\frac{y^2}{2}-\frac{y^3}{6}\right) + \left(M+\frac{1}{Da}\right)\left(\frac{y^2}{2}-\frac{y^3}{6}\right) + \left[\frac{Gre}{3} - \frac{1}{3}\left(M+\frac{1}{Da}\right) - \frac{1}{2}\frac{dp}{dx}\right] y \tag{30}$$

$$T_1 = S\left(\frac{y^2}{2}-\frac{y^3}{6}\right) - Br\frac{y^2}{2} + \left[\frac{Br}{2} - \frac{S}{3}\right] y \tag{31}$$

For the 2nd order, Eqs. (17) and (22) are solved as:

$$\begin{aligned} u_2 = {} & -GreS\left(\frac{y^4}{24}-\frac{y^5}{120}\right) - \frac{GreBry^3}{12} + \frac{GreSy^3}{18} + \frac{GreBry^4}{24} \\ & + \left(M+\frac{1}{Da}\right)\left[\frac{y^4}{24}\frac{dp}{dx} - Gre\left(\frac{y^4}{24}-\frac{y^5}{120}\right) + \left(M+\frac{1}{Da}\right)\left(\frac{y^4}{24}-\frac{y^5}{120}\right) + \frac{Grey^3}{18} + \frac{\left(M+\frac{1}{Da}\right)y^3}{18} - \frac{y^3}{12}\frac{dp}{dx}\right] + A_5 y + A_6 \end{aligned} \tag{32}$$

$$T_2 = S\left[\left(\frac{Sy^4}{24}-\frac{Sy^5}{120}\right)-Br\frac{y^4}{24}+\left[\frac{Br}{2}-\frac{S}{3}\right]\frac{y^3}{6}\right]$$

$$-2Br\left[-\frac{y^3}{6}\frac{dp}{dx}+Gre\left(\frac{y^3}{6}-\frac{y^4}{24}\right)-\left(M+\frac{1}{Da}\right)\left(\frac{y^3}{6}-\frac{y^4}{24}\right)-\frac{Grey^2}{6}+\frac{\left(M+\frac{1}{Da}\right)y^2}{6}+\frac{y^2}{4}\frac{dp}{dx}\right]B_5 y+B_6 \tag{33}$$

Applying boundary conditions $\mathrm{u}_2(0)=0$, $\mathrm{u}_2(1)=0$ and $T_2(0)=0$, $T_2(1)=0$

$$A_5=\frac{GreBr}{24}-\frac{GreS}{45}-\left(M+\frac{1}{Da}\right)\left(\frac{Gre}{45}-\frac{\left(M+\frac{1}{Da}\right)}{45}-\frac{1}{24}\frac{dp}{dx}\right), \tag{34}$$

$$A_6=0$$

$$B_5=2Br\left[-\frac{1}{6}\frac{dp}{dx}+\frac{Gre}{8}-\frac{\left(M+\frac{1}{Da}\right)}{8}-\frac{Gre}{6}+\frac{\left(M+\frac{1}{Da}\right)}{6}+\frac{1}{4}\frac{dp}{dx}\right]-\frac{S^2}{30}-\left(\frac{SBr}{12}-\frac{S^2}{18}\right)+\frac{SBr}{24}, \tag{35}$$

$$B_6=0$$

Therefore, the approximate solutions of Eqs. (7) and (8) are:

$$u=u_0+u_1+u_2+\cdots \tag{36}$$

$$T=T_0+T_1+T_2+\cdots \tag{37}$$

The physical quantities of interest are reverse flow, pressure gradient, skin friction, and rate of heat transfer on the plate surfaces. To obtain the pressure gradient $\frac{dP}{dx}$ of the flow assuming a uniform mass flux q, we integrate u from 0 to 1 with respect to y.

$$\int_0^1 u dy = q \tag{38}$$

and obtain the pressure gradient as:

$$\frac{dP}{dx}=\frac{\left(-q+\frac{1}{2}+\frac{Gre}{24}-\frac{\left(M+\frac{1}{Da}\right)}{24}+\frac{5GreS}{720}+\frac{GreBr}{120}-\frac{\left(M+\frac{1}{Da}\right)Gre}{240}+\frac{\left(M+\frac{1}{Da}\right)^2}{240}-\frac{GreS}{90}\right)}{\left(\frac{1}{2}-\frac{\left(M+\frac{1}{Da}\right)}{120}\right)} \tag{39}$$

The skin friction (Sk) on both the plates expressed as coefficient of surface skin stress is given by:

$$\mathrm{Sk}_{(0,1)}=\frac{du}{dy}\Big|_{(y=0,1)} \tag{40}$$

while the rate of heat transfer expressed as local Nusselt number Nu at both the plates are given by:

$$\mathrm{Nu}_{(0,1)} = \frac{dT}{dy}\Big|_{(y=0,1)} \tag{41}$$

Numerical solution

The Eqs. (5) and (6) subject to Eq. (7) are solved numerically using implicit finite difference method.

Implicit finite difference scheme

$$-r\boldsymbol{u}_{i-1}^{j+1} + (1+2r)\boldsymbol{u}_{i}^{j+1} - r\boldsymbol{u}_{i+1}^{j+1} = (1-r_1)\boldsymbol{u}_{i}^{j} + Gre\Delta t\boldsymbol{T}_{i}^{j} + \lambda\Delta t \tag{42}$$

$$-r\boldsymbol{T}_{i-1}^{j+1} + (\mathrm{Pr}+2r)\boldsymbol{T}_{i}^{j+1} - r\boldsymbol{T}_{i+1}^{j+1} = (\mathrm{Pr}-S\Delta t)\boldsymbol{T}_{i}^{j} + r_2\left(\boldsymbol{u}_{i+1}^{j} - \boldsymbol{u}_{i-1}^{j}\right)^2 \tag{43}$$

where, $r = \left(\frac{\Delta t}{\Delta y}\right)^2$, $r_1 = \Delta t\left(\mathrm{M} + \frac{1}{Da}\right)$ *and* $r_2 = \frac{\mathrm{B}r}{4}\left(\frac{\Delta t}{\Delta y}\right)^2$

Results and discussion

The transient mixed convective Couette flow of viscous dissipative fluid in a channel filled with porous material are theoretically studied. One of the plate moves in the direction of the fluid flow, while the other plate is stationary. The influences of the governing flow parameters are presented in graphs and tables. For the purpose of discussion, the values of the parameters that govern the flow are carefully selected to represent realistic parameters of some real fluids. In this work, we considered air to be the working fluid with the following as default values:

$$\left(Gre = 50,\ S = 0.2,\ Br = 0.01,\ \mathrm{Pr} = 0.71,\ M = 1,\ Da = 0.1\right)$$

unless otherwise stated, while S < 0 and S > 0 signifies heat generation and absorption respectively. The skin friction and the rate of heat transfer on the fluid-plate interface are tabulated in **Tables 1** to **4**, for S, Br, Da and M, respectively.

Figures 2(a) and **2(b)** describe the influence of Br on velocity and temperature profile respectively, it is evident from **Figures 2(a)** and 2**(b)** that increase in Br rises the fluid flow **Figures 3(a)** and **3(b)** illustrate the effect of Darcy parameter (Da) and Magnetic field (M) on velocity profile. From **Figure 3(a)**, it is observed that the velocity increases with increasing Da. This is physically true, when fluid material moved in quantity, more viscous energy is generated which causes an increase in fluid boundary layer and thickness thereby leading to an enhancement in fluid velocity, but the reversed is observed at lower part of the plate when the plate is cool. It is evident from **Figure 3(b)** that increase in M decreases the velocity fluid flow. **Figures 4(a)** and **4(b)** show the positive and negative effect of mixed convection parameter (Gre) on velocity profile, **Figure 4(a)** revealed that the velocity profile increases near the heated plate with increase in mixed convection parameter, a significant increase was noticed when the thermal buoyancy forces increases, the heat energy diffuses easily and makes the fluid less dense, thus fluid flow increases. It is also observed that the thickness of the velocity profile boundary layers decreases at the upper part of the heated plate with increase in thermal buoyancy at $Gre > 0$, while the reversed case was noticed at the center. This attributed to the fact that the fluid is dense near the cold plate. This is physically seen, when the energy dissipated by viscous dissipation and heat conducted by the heated plate diffuses by the thermal buoyancy forces thereby increases the velocity fluid flow, and reversed case is presented in **Figure 4(b)** at $Gre < 0$.

The impact of the Prandtl number Pr is displayed in **Figures 5(a)** and **5(b)** as it can be seen that, increasing Pr leads to decrease in both temperature and velocity significantly, this is because increasing this parameter means to reduce the fluid's thermal conductivity which reduces the rate at which heat is transported from the heated channel walls into the fluid flow. It is also observed from 5b that, the boundary layer thickness is high than that of velocity profile (**Figure 5(a)**) which indicates the rate of heat transfer is strongly high in **Figure 5(b)** than in **Figure 5(a)**. **Figures 6(a)** and b presents the effect of heat source/sink (S) on Velocity and Temperature Profiles respectively, in both **Figures 6(a)** and **6(b)** a significant decrease was observed due to the increase in heat absorption $S > 0$, which implies source/sink (S) deceases the temperature and velocity fluid flow in this research work. **Table 1**. Illustrate the effects of heat source/sink

parameter (*S*) on the frictional force and the rate of heat transfer when other parameters are kept constant. It is evident that growing levels of heat source increase the skin friction at $y = 0$ whereas a reverse case is recorded at the cold plate $y = 1$. Additionally, rate of heat transfer is enhanced at $y = 0$ while an oppose phenomenon occurs at $y = 1$.

The influence of Br on the shear stress and heat transfer rate is demonstrated in **Table 2**. As other parameters are maintained at constant values. Higher values of Br are seen to boost the skin friction at the heated plate while a revers situation is observed at $y = 1$. Similarly, the rate of heat transfer is improved for rising levels of Br, whereas an opposite case is seen to occur at $y = 1$. **Table 3** depicts the impact of Darcy (*Da*) on the heated and cold plates ($y = 0$, and $y = 1$, respectively) when other parameters are taken constants values. It is clear that increasing values of *Da* leads to a dramatic increase in the frictional force at the plate $y = 0$, whereas at the cold plate, a reverse phenomenon is demonstrated. The effect of *M* when other parameters are kept constant, on the skin friction is displayed in **Table 4**. It is obvious that greater values of *M* is seen to upsurge the shear stress at the heated plate while an opposite situation occurs at the cold plate $y = 1$.

Table 1 Presents the effect of skin friction and Nusselt number on the heated and cold plate (y = 0 and y = 1, respectively) for heat source/sink parameter (*S*) at *Gre* = 100, *Br* = 0.01, *Da* = 0.01, *M* = 1, t = 0.01, Pr = 0.71.

S	$\tau_0(-)$	τ_1	$\mathrm{N}u_0(-)$	$\mathrm{N}u_1$
−0.3	0.4089	0.4126	0.4124	0.3685
−0.2	0.4186	0.4068	0.4260	0.3624
−0.1	0.4282	0.4011	0.4394	0.3563
0.3	0.4652	0.3794	0.4914	0.3350
0.2	0.4562	0.3846	0.4786	0.3391
0.1	0.4470	0.3900	0.4657	0.3447

Table 2 Shows the effect of skin friction and Nussle number at the heated and cold plate (y = 0 and y = 1, respectively) for *Br* at *Gre* = 100, *Da* = 0.01, *M* = 1, *S* = 2, Pr = 0.71, t = 0.01.

Br	$\tau_0(-)$	τ_1	$\mathrm{N}u_0(-)$	$\mathrm{N}u_1$
0.01	0.6007	0.3051	0.6871	0.2559
0.03	0.6785	0.2517	0.7965	0.1921
0.05	0.7611	0.2049	0.9174	0.1391

Table 3 Shows the effect of skin friction and Nussle number at the heated and cold plate (y = 0 and y = 1 respectively) for *Da* at *Gre* = 100, *Br* = 0.01, *Br* = 0.01, *M* = 1, S = 2, Pr = 0.71, t = 0.01.

Da	τ_0	τ_1
0.01	–0.6007	0.3051
0.02	0.0016	0.0006
0.03	0.0029	0.0008
0.05	0.0044	0.0012

Table 4 Shows the skin friction and Nussle number at the heated and cold plate (y = 0 and y = 1 respectively) for *M* at *Gre* = 100, *Br* = 0.01, *Br* = 0.01, *Da* = 0.0 1, *S* = 3, Pr = 0.71, t = 0.01.

M	$\tau_0(-)$	τ_1
0.1	0.6376	0.2738
0.3	0.6443	0.2733
0.5	0.6510	0.2728
0.7	0.6643	0.2719

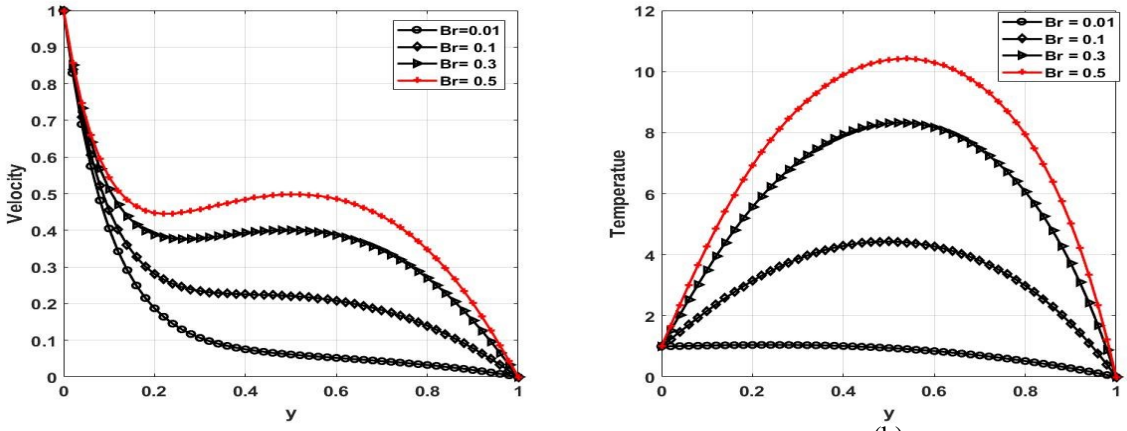

(a) (b)

Figure 2 Velocity and temperature profile for brinkman number (*Br*) at (*Gre* = 5, *Da* = 0.01, *Mg* = 1, *S* = 2, Pr = 0.71).

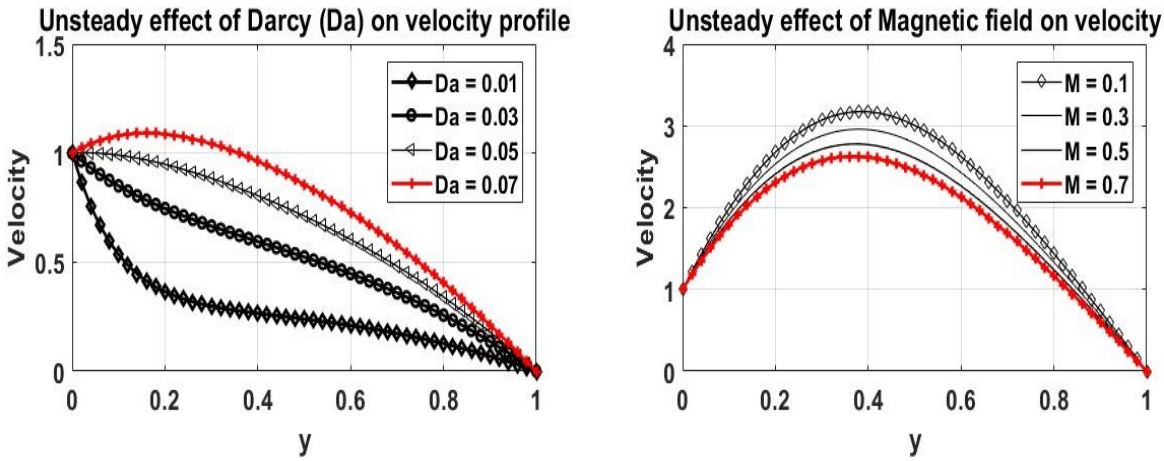

(a) (b)

Figure 3 Comparison of the effect of magnetic field (*M*) and Darcy parameter on velocity profile at (*Gre* = 25, *S* = 0.2, *Br* = 0.01, Pr = 0.71, *M* = 1) and (*Gre* = 40, *S* = 0.2, *Br* = 0.01, Pr = 0.71, *Da* = 0.1), respectively.

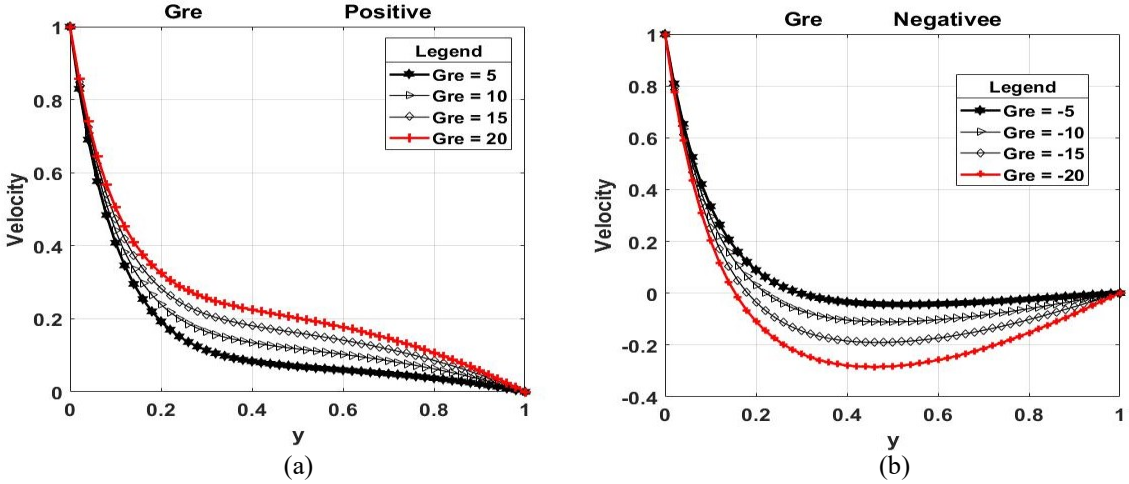

(a) (b)

Figure 4 Effect of mixed convection parameter (*Gre*) on velocity profile at (*Br* = 0.01, *Da* = 0.01, *Mg* = 1, *S* = 0.2, Pr = 0.71).

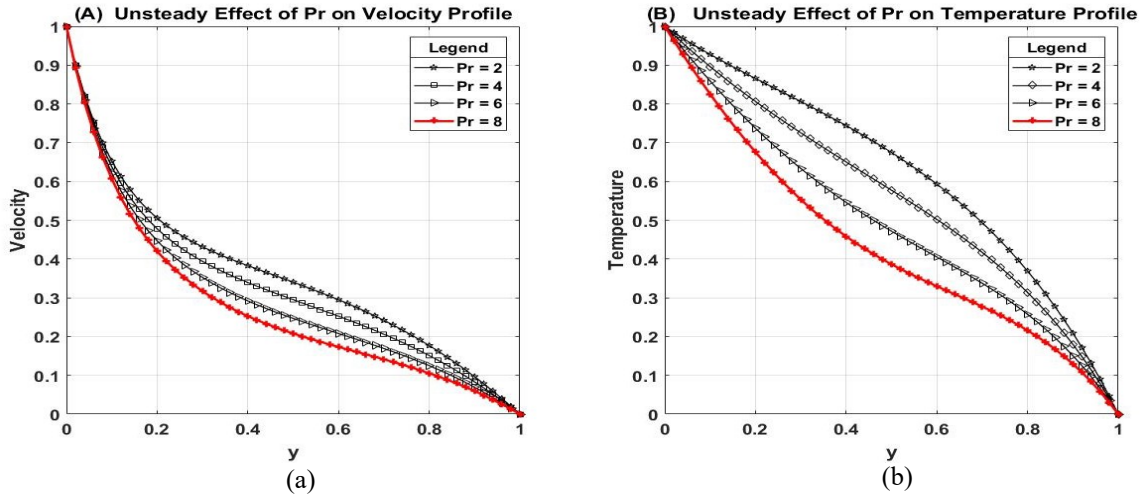

(a) (b)

Figure 5 Effect of Prandlt number (Pr) on velocity and temperature profile at $(Gre = 50, Da = 0.01, Mg = 1, S = 2, Br = 0.01)$ Pr =2, 4, 6, 8.

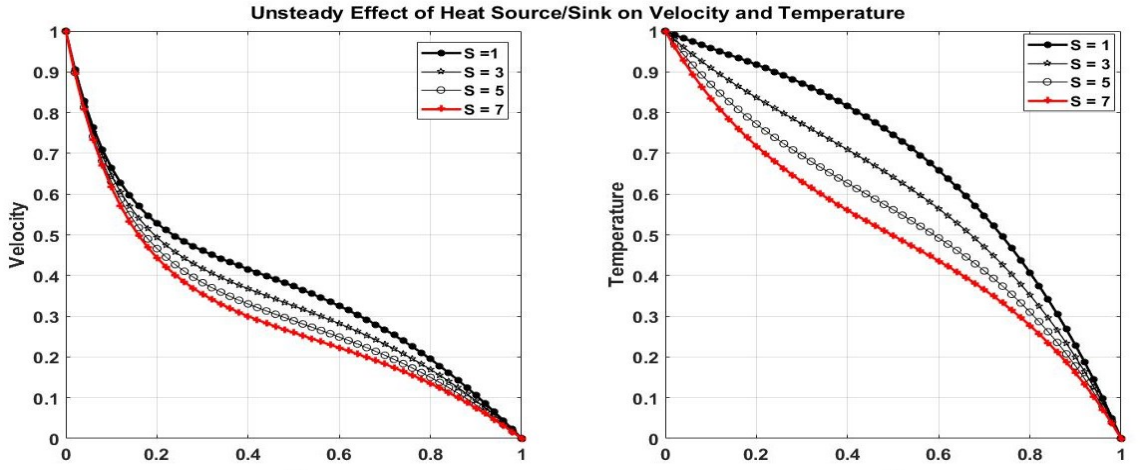

(a) (b)

Figure 6 Effect of heat source/sink (S) on velocity and temperature profile at (Gre = 50, Mg = 1, Da = 0.01, Br = 0.01, Pr = 0.71).

Conclusions

This work is dedicated to the examination of unsteady MHD mixed convective flow of viscous dissipation of fluid in a channel filled with porous material. The steady state analytical solutions of energy, momentum as well as frictional factor, and heat transfer rate are obtained using the Homotopy perturbation method. The time-dependent controlling equations are numerically solved using an implicit finite difference scheme, and the impact of dimensionless regulating parameters and dynamic flows is explained and displayed in graphs and tables. While the implicit solution is assumed to be attained at relatively large time increments, the iteration procedure and calculations of the inverse stiffness matrix make the computations rather expensive in terms of memory, disk space, and computational time. On the other hand, the implicit finite difference methods have some major advantages which include the stability of the scheme, the computational of discontinuities (e.g. hydraulic jump), the calculation of the boundary conditions and the variable spatial interval. According to the results, increasing the values of *Gre*, *Br*, and *Da* improves the fluid velocity whereas increasing the values of *M* and Pr has the opposite effect on the flow pattern. This research has applications in the lubrication industries and biomedical sciences and has proved very useful to designers in increasing the performance of mechanical systems when viscous dissipation is involved.

References

[1] M Avci and O Aydin. Mixed convection in a vertical parallel plate microchannel with asymmetric WallHeat fluxes. *J. Heat Transfer.* 2017; **129**, 1091-5.

[2] A Avramenko, AI Tyrinov, IV Shevchuk, NP Dmitrenko, AV Kravchuk and IV Shevchuk. Mixedconvection in a vertical flat microchannel. *Int. J. Heat Mass Tran.* 2017; **106**, 1164-73.

[3] BK Jha, S Gabriel and PB Malgwi. Adomian decomposition method for combined effect of hall and ion-slip on mixed convection flow of chemically reacting newtonian fluid in a micro-channel with heat absorption/generation. *Int. J. Modern Phys. C* 2020; **31**, 2050150.

[4] K Khanafera, MS Aithal and K Vafaid. Mixed convection heat transfer in a differentially heated cavity with two rotating cylinders. *Int. J. Therm. Sci.* 2019; **135**, 117-32.

[5] VG Gupta, J Ajay and A Kumar. Mixed convection flow of viscous dissipating fluid through channel moving in opposite direction. *IOSR J. Math.* 2016; **12**, 50-9.

[6] Z Masoud, T Davood and A Karimipour. Developing a new correlation to estimate the thermal conductivity of MWCNT-CuO/water hybrid nanofluid via an experimental investigation. *J. Therm. Anal. Calorim.* 2017; **129**, 859-67.

[7] H Xu and Q Sun. Generalized hybrid nanofluid model with the application of fully developed mixed convection flow in a vertical microchannel. *Commun. Theor. Phys.* 2019; **71**, 903-11.

[8] E Manay and E Mandev. Experimental investigation of mixed convection heat transfer of nanofluids in a circular microchannel with different inclination angles. *J. Therm. Anal. Calorim*. 2019; **135**, 887-900.

[9] B Gebhart. Effect of viscous dissipation in natural convection. *J. Fluid. Mech.* 1962; **14**, 225-32.

[10] OA Ajibade and MU Ayuba. Effects of viscous dissipation on a steady mixed convection Couette flow of heat generating/absorbing fluid. *J. Pure Appl. Sci.* 2021; **21**, 67-7668.

[11] OA Ajibade and MU Ayuba. An analytical study on effect of viscous dissipation and suction/injection on a steady MHD natural convection couette flow of heat generation/absorbing fluid. *Adv. Mech. Eng.* 2021; **13**, 1-12.

[12] BK Jha and OA Ajibade. Effect of viscous dissipation on natural convection flow between vertical parallel plates with time-periodic boundary conditions. *Commun. Nonlin. Sci. Numer. Simul.* 2012; **17**, 1576-87.

[13] BK Jha, D Daramola and OA Ajibade. Mixed convection in an inclined channel filled with porous material having time-periodic boundary conditions: steady-periodic regime. *Trans. Porous Media* 2015; **2**, 495-512.

[14] OA Ajibade and UO Thomas. Entropy generation and irrevers-ibility analysis due to steady mixed convection flow in a vertical porous channel. *Int. J. Heat Tech.* 2017; **35**, 433-46.

[15] A Mohamed. Mixed convection flow of a micropolar fluid from an unsteady stretching surface with viscous dissipation. *J. Egypt. Math. Soc.* 2013; **21**, 385-94.

[16] A Mohamed. Unsteady mixed convection heat transfer along a vertical stretching surface with variable viscosity and viscous dissipation. *J. Egypt. Math. Soc.* 2014; **22**, 529-37.

[17] P Dulal and M Hiranmony. Effects of temperature-dependent viscosity and variable thermal conductivity on MHD non-darcy mixed convective diffusion of species over a stretching sheet. *J. Egypt. Math. Soc.* 2014; **22**, 123-33.

[18] Y Mahmoudi, K Hooman and K Vafai. Convective heat transfer in porous media. Taylor & Francis Group, LLC CRC Press, New York, 2020, p. 397.

[19] Y Joshi and B Gebhart. Mixed convection in porous media adjacent to a vertical uniform heat flux surface. *Int. J. Heat Mass Tran.* 1985; **28**, 1783-6.

[20] A Chamkha, RS Gorla and K Ghodeswar. Non-similar solution for natural convective boundary layer flow over a sphere embedded in a porous medium saturated with a nano fluid. *Transport Porous Media* 2011; **86**, 13-22.

[21] AJ Chamkha. Mixed convection flow along a vertical permeable plate embedded in a porous medium in the presence of a transverse magnetic field. *Numer. Heat Tran. A Appl*. 2007; **34**, 93-103.

[22] BJ Gireesha and S Sindhu. MHD natural convection flow of casson fluid in an annular microchannel containing porous medium with heat generation/absorption. *Nonlinear Eng.* 2020; **9**, 223-32.

[23] N Alam, S Poddar, ME Karim, MS Hasan and G Lorenzini. Transient MHD radiative fluid flow over an inclined porous plate with thermal and mass diffusion: An EFDM numerical approach. *Math. Model. Eng. Probl.* 2021; **8**, 739-49.

[24] JH He. Homotopy perturbation method for solving boundary value problems. *Phys. Lett. A* 2006; **350**, 87-8.

[25] JH He. A coupling method of a homotopy perturbation technique and a perturbation technique for non-linear problems. *Int. J. Non-Linear Mech.* 2000; **35**, 37-43.
[26] JH He. Homotopy perturbation method: a new nonlinear analytical technique. *Appl. Math. Comput.* 2003; **135**, 73-9.
[27] B Zigta. Mixed convection on MHD flow with thermal radiation, chemical reaction and viscous dissipation embedded in a porous medium. *Int. J. Appl. Mech. Eng.* 2020; **25**, 219-35.